

## Quasiselection rules for multiphonon absorption in alkali halides\*

C. J. Duthler

*Xonics, Incorporated, Van Nuys, California 91406*

(Received 12 April 1976)

A quasiselection rule is derived that multiphonon infrared absorption in alkali halides prefers final states containing an odd number of optical phonons. This quasiselection rule explains the recent observation of a well-defined peak in the low-temperature infrared absorption of several alkali halides at a frequency corresponding to the sum of three optical phonons. No corresponding peak occurs at the two- or four-optical-phonon summation-band frequencies. It is shown that the quasiselection rule results from the relative ionic displacements for optical modes being approximately in phase with the individual ion displacements, while the relative ionic displacements for acoustical modes are approximately  $90^\circ$  out of phase. The further realization that, at least for optical modes, the magnitude of the Fourier-transformed relative displacement is nearly independent of the phonon wave number greatly reduces the effort of the calculation. This approximation reduces an extremely tedious momentum-dependent sum to a thermally and frequency weighted density of states in which the phonon branches are kept distinct.

### I. INTRODUCTION

The advent of high-power infrared lasers has stimulated considerable recent interest in the small amount of absorption of transparent solids in the far wings of their infrared absorption bands.<sup>1</sup> In alkali halides at frequencies greater than approximately twice the fundamental reststrahl frequency, the absorption coefficient  $\beta$  is observed to decrease exponentially with increasing frequency.<sup>2</sup> Until recently no structure has been observed in the high-frequency, multiphonon region. Recent experiments by Harrington *et al.*<sup>3</sup> at low temperature (80 K) show a well-defined peak in the absorption coefficient of several alkali halides at a frequency corresponding to the sum of three optical phonons. No corresponding peak is observed at the two- or four-optical-phonon summation frequencies and the three-optical-phonon summation band is observed to be most pronounced in crystals having a large mass ratio between the heavy and light crystal ions. These observations suggest an odd-even selection rule that allows odd-numbered optical-phonon summation bands. Such a selection rule is derived in this paper and is called a quasiselection rule since it is approximate (unallowed transition-matrix elements small, but nonzero).

Previous theories<sup>4-9</sup> generally predict a smoothly exponentially decreasing absorption coefficient in the multiphonon region in agreement with previous room-temperature experiments. Structure in the multiphonon absorption coefficient can arise from structure in both the multiphonon density of states and transition-matrix elements. Evidence is presented in the present paper that much of the fine-scale structure in the multiphonon density of states is smoothed out by the short lifetime, hence large

spectral width, of the final-state optical phonons at room temperature. The remaining broad structure observed by Harrington *et al.*<sup>3</sup> is shown to result from transition-matrix elements which favor transitions to final states containing an odd number of optical phonons.

Many past theories treat the lattice as a set of molecular oscillators on which a density of states is impressed. Such past theories have neglected the suppression of even-numbered optical-phonon summation bands and any structure in the absorption coefficient, if predicted, occurs at both even- and odd-numbered combinations.

The present paper is based on a perturbation-theory calculation on actual crystal phonons by Sparks and Sham.<sup>4</sup> An error in the Sparks and Sham<sup>4</sup> paper is corrected which, when corrected, leads to multiphonon quasiselection rules. Further reasonable approximations greatly simplify the otherwise very tedious perturbation-theory calculation.

Previously, selection rules were derived for the two-phonon region. An exact group-theory selection rule forbids final-state phonons on the same phonon branch.<sup>10,11</sup> Subsequently Duthler and Sparks<sup>12</sup> derived a two-phonon quasiselection rule which favors final states consisting of an optical plus an acoustical phonon over final states consisting of two optical or two acoustical phonons. This quasiselection rule yields four quasiallowed combinations of phonon bands: TA + TO, LA + TO, TA + LO, and LA + LO, where O and A denote optical and acoustical branches, and T and L denote transverse and longitudinal. Typically four two-phonon absorption peaks are observed in alkali halides<sup>13</sup> in agreement with the quasiselection rule and in contrast with numerous additional peaks possible from the joint density of states. Eldridge

and co-workers<sup>14</sup> have examined the absorption peaks in LiF in detail. Strong two-phonon summation peaks were traced to the combination of branches and the particular region of the Brillouin zone contributing to the peak. Four strong contributions were found for combinations of optical plus acoustical branches, although branch identification is somewhat difficult in LiF due to dispersion curve crossings.

## II. ABSORPTION MECHANISM

There are two possible mechanisms for multiphonon infrared absorption in dielectric crystals: In the higher-order-dipole-moment mechanism the absorbed photon directly creates  $n$  final-state phonons, as is illustrated in Fig. 1(a). In the anharmonic lattice mechanism only the fundamental reststrahl (TO, zero momentum) phonon couples to the radiation field. In this case illustrated in Fig. 1(b), the intermediate-state reststrahl phonon is driven off resonance and decays into  $n$  final-state phonons. It was previously thought that the anharmonic lattice mechanism is dominant in alkali halides, although this is now questioned especially at large  $n$ .<sup>15</sup> The leading terms in the transition-matrix elements for the two mechanisms are expected to be similar<sup>16,17</sup> with the result that the quasiselection rules derived in Sec. III for the

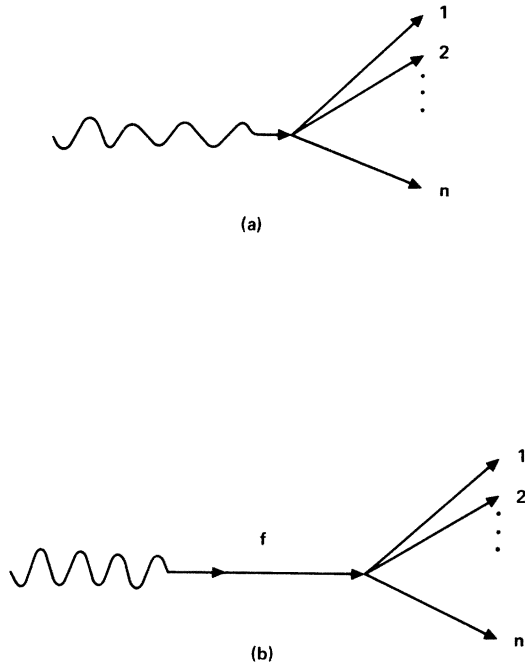


FIG. 1. (a) In the higher-order-dipole-moment mechanism the absorbed photon directly creates  $n$  final-state phonons. (b) Only the fundamental reststrahl phonon couples to the radiation field in the anharmonic lattice mechanism.

anharmonic lattice mechanism should also be valid for the higher-order-dipole-moment mechanism.

To illustrate the equivalent functional form of the leading terms of the two mechanisms, consider the interaction Hamiltonian for radiation absorption by the anharmonic lattice mechanism. Assuming a central-force lattice potential, the  $n$ -phonon anharmonic lattice interaction Hamiltonian is proportional to the  $n$ th power of the relative displacement of ion pairs:

$$\mathcal{H}_{\text{anh}}^{(n)} \propto \sum_l \sum_m (\hat{\delta}_{lm} \cdot \vec{u}_{lm})^n (\hat{u}_f \cdot \hat{\delta}_{lm}). \quad (2.1)$$

Here  $\vec{u}_{lm} = \vec{u}_l - \vec{u}_m$ , where  $\vec{u}_l$  and  $\vec{u}_m$  are the displacements of the  $l$ th and  $m$ th ions from equilibrium. The unit vector  $\hat{\delta}_{lm}$  is directed from the equilibrium positions of the  $l$ th ion to the  $m$ th ion and  $\hat{u}_f$  is the unit polarization vector for the ion motion in the fundamental mode.

In rock-salt structure crystals the absorption coefficient is independent of the direction of propagation. Choosing the  $x$  direction for the radiation polarization ( $\hat{u}_f = \hat{x}$ ) and keeping only the nearest neighbors in the summation, Eq. (2.1) becomes

$$\mathcal{H}_{\text{anh}}^{(n)} \propto \sum_l \sum_{m=\pm x} (\hat{\delta}_{lm} \cdot \vec{u}_{lm})^n, \quad (2.2)$$

where now  $l$  labels the light ion in the unit cells and the sum on  $m$  is restricted to nearest neighbors at  $\pm a_{nm} \hat{x}$ . The multiphonon quasiselection rule is derived from the term under the summation with the relative ionic displacement expressed in terms of crystalline normal modes.

It is reasonable to expect that the higher-order dipole moment which arises from the  $n$ th power of the relative ionic displacement is dominated by contributions of nearest-neighbor pairs and is directed along the line connecting the ion centers. If these conditions are satisfied, at least the leading terms of the interaction Hamiltonian for the higher-order-dipole-moment mechanism have the same form as Eq. (2.2) for radiation polarized in the  $x$  direction. The leading terms of the two mechanisms differ only in the proportionality constant. Reasonable estimates can be made for the proportionality constant of the anharmonic lattice mechanism from the  $(n+1)$ th derivative of model potentials, but the proportionality constant for the higher-order-dipole-moment mechanism is highly uncertain.

## III. DERIVATION OF QUASISELECTION RULE

The infrared dielectric constant for the anharmonic lattice mechanism is

$$\epsilon(\omega) = \epsilon_\infty + (\epsilon_0 - \epsilon_\infty) \omega_f^2 / [\omega^2 - \omega_f^2 - i\omega_f \Gamma(\omega)], \quad (3.1)$$

where  $\epsilon_0$  and  $\epsilon_\infty$  are the static and high-frequency dielectric constants,  $\omega_f$  is the frequency of the fundamental reststrahl mode, and  $\Gamma(\omega)$  is the frequency-dependent relaxation frequency of the fundamental mode. The absorption coefficient is given by  $\beta = k_0 \epsilon_f / n_R$ , where  $k_0$  is the vacuum propagation constant of the radiation,  $\epsilon_f$  is the imaginary part of the dielectric constant, and  $n_R$  is the real part of the refractive index  $n = \epsilon^{1/2}$ . For

$$\Gamma_n(\omega) = \frac{2\pi}{\hbar} (n+1)^2 n! \sum_{Q_1, \dots, Q_n} |\Lambda(fQ_1, \dots, Q_n)|^2 \Delta \left( \sum_{j=1}^n \vec{q}_j \right) \delta \left( \omega - \sum_{j=1}^n \omega_{Q_j} \right) \bar{n}_n, \quad (3.2)$$

where  $Q$  denotes the phonon mode having wave vector  $\vec{q}$ , branch  $b$  and frequency  $\omega_Q$ ;  $\Delta$  is the modified Kronecker  $\delta$  which is unity when the argument is zero or a reciprocal-lattice vector and zero otherwise; and

$$\bar{n}_n = \prod_{j=1}^n \frac{n_{Q_j} + 1}{n_\omega + 1}, \quad (3.3)$$

where  $n_Q$  and  $n_\omega$  are Bose-Einstein occupation numbers of the phonon mode  $Q$  and frequency  $\omega$ , respectively.

The total renormalized vertex  $\Lambda(fQ_1, \dots, Q_n)$  is approximated by the simple vertex  $V(fQ_1, \dots, Q_n)$  multiplied by a vertex renormalization factor

$$\Lambda(fQ_1, \dots, Q_n) = \Lambda_n V(fQ_1, \dots, Q_n). \quad (3.4)$$

The simple vertex  $V(Q_1, \dots, Q_m)$  involves all derivatives of the potential through order  $m$ , but no products of derivatives as does the renormalized vertex. Sparks and Sham<sup>4</sup> justify retaining only the  $m$ th-order derivative of the assumed nearest-neighbor, central-force potential  $\phi^{(m)} = d^m \phi / dr^m$ , and obtain

$$V(Q_1, \dots, Q_m) = \frac{N}{m!} \phi^{(m)} \sum_{\gamma=1}^6 \prod_{j=1}^m U_\gamma(Q_j) \left( \frac{\hbar}{2Nm_\zeta \omega_{Q_j}} \right)^{1/2}, \quad (3.5)$$

where  $N$  is the number of unit cells in the crystal and  $m_\zeta$  is the mass of the light ion in the unit cell. The sum on  $\gamma$  runs over the nearest-neighbor heavy ions which, in rock-salt structure crystals, are located at the six positions  $\pm a_m \hat{x}$ ,  $\pm a_m \hat{y}$ , and  $\pm a_m \hat{z}$  from each light ion with the directions to these positions being given by the unit vectors  $\hat{x}_\gamma$ . The quantity

frequencies away from the resonant frequency, peaks in the relaxation frequency will be reflected in peaks in the absorption coefficient.

Sparks and Sham<sup>4</sup> have derived formal expressions for the relaxation frequency using the perturbation-theory result that the probability per unit time of a transition between two states is  $2\pi/\hbar$  times the square of the transition-matrix element. The total relaxation frequency of the fundamental mode is the sum of processes involving all numbers of phonons with the contribution from the  $n$ -phonon summation process shown in Fig. 1(b) being

$$U_\gamma(Q) = \hat{x}_\gamma \cdot [\vec{w}_{<Q_j} - (m_{<}/m_{>})^{1/2} \vec{w}_{>Q_j} e^{i\vec{q} \cdot \hat{x}_\gamma a_{nn}}] \quad (3.6)$$

is the  $\hat{x}_\gamma$  component of the Fourier-transformed relative displacement of the light ion from the heavy ion located at  $\hat{x}_\gamma a_{nn}$ . The polarization vectors  $\vec{w}_{<Q}$  and  $\vec{w}_{>Q}$  are implicitly defined by the equation expressing the displacement  $\vec{u}_{I\tau}$  of an ion from its equilibrium position  $\vec{x}_{I\tau}$  in terms of phonon modes:

$$\vec{u}_{I\tau} = \sum_Q \left( \frac{\hbar}{2Nm_\tau \omega_Q} \right)^{1/2} e^{i\vec{q} \cdot \vec{x}_{I\tau}} A_Q \vec{w}_{\tau Q}, \quad (3.7)$$

where  $\tau$  denotes the ion type and  $A_Q = a_Q + a_{-Q}^\dagger$ , with  $a_Q$  and  $a_{-Q}^\dagger$  being phonon creation and annihilation operators. With the convention used in writing Eq. (3.7), the components of the polarization vectors  $\vec{w}_{\tau Q}$  are real numbers.

For the fundamental reststrahl mode, the Fourier-transformed relative displacement in Eq. (3.6) becomes

$$U_\gamma(f) = \hat{x}_\gamma \cdot \hat{w}_f (m_{<}/m_r)^{1/2}, \quad (3.8)$$

where  $m_r$  is the reduced mass of the two ions in a unit cell.

Substituting this result for one of the phonon modes in Eq. (3.5) and using Eqs. (3.3) and (3.4), the relaxation frequency in Eq. (3.2) can be written

$$\Gamma_n(\omega) = \frac{2\pi}{\hbar^2} \frac{1}{n!} \left( \frac{\hbar}{2m_\zeta} \right)^{n+1} \left( \frac{m_\zeta}{m_r} \right) \times \omega^{-1} (n_\omega + 1)^{-1} (\phi^{(n+1)})^2 \Lambda_n^2 \Sigma_n, \quad (3.9)$$

where the dynamical information of the phonons is contained in  $\Sigma_n$ :

$$\Sigma_n = \sum_{\gamma=1}^6 \sum_{\gamma'=1}^6 (\hat{x}_\gamma \cdot \hat{w}_\gamma) (\hat{x}_{\gamma'} \cdot \hat{w}_{\gamma'}) N^{-n} \sum_{Q_1, \dots, Q_n} N \Delta \left( \sum_{j=1}^n \vec{q}_j \right) \delta \left( \omega - \sum_{j=1}^n \omega_{Q_j} \right) \prod_{j=1}^n U_\gamma(Q_j) U_{\gamma'}^*(Q_j) \omega_{Q_j}^{-1} (n_{Q_j} + 1). \quad (3.10)$$

This result for  $\Sigma_n$  is identical to that given in Eq. (2.21) of Sparks and Sham.<sup>4</sup> In going from their Eq. (2.21) to Eq. (2.24) Sparks and Sham<sup>4</sup> made an algebraic error when expressing  $\Sigma_n$  in terms of real and imaginary parts of  $U_x(Q)$ . Rather than simply correcting the algebra in Ref. 4, a different approach is taken from this point on in the present paper.

In rock-salt structure crystals the absorption is independent of the direction of propagation. Hence, for convenience we choose  $\hat{\omega}_f = \hat{x}$ . With this choice the only terms surviving the sums over nearest neighbors in Eq. (3.10) are those located at  $\pm \hat{x}a_{nn}$ . Interchanging sums on  $\gamma$  and  $Q$ , Eq. (3.10) becomes

$$\Sigma_n = N^{-n} \sum_{Q_1, \dots, Q_n} N\Delta \left( \sum_{j=1}^n \vec{q}_j \right) \delta \left( \omega - \sum_{j=1}^n \omega_{Q_j} \right) \sum_{\gamma = \pm x} \sum_{\gamma' = \pm x} (\hat{x}_\gamma \cdot \hat{x}) (\hat{x}_{\gamma'} \cdot \hat{x}) \prod_{j=1}^n U_\gamma(Q_j) U_{\gamma'}^*(Q_j) \omega_{Q_j}^{-1} (n_{Q_j} + 1). \quad (3.11)$$

An examination of Eq. (3.6) reveals that the components of the Fourier-transformed relative displacements in the positive and negative  $x$  directions are related by

$$U_{-x}(Q) = -U_x^*(Q). \quad (3.12)$$

Using this result in the sums on  $\gamma$ , Eq. (3.11) can be written

$$\Sigma_n = N^{-n} \sum_{Q_1, \dots, Q_n} N\Delta \left( \sum_{j=1}^n \vec{q}_j \right) \delta \left( \omega - \sum_{j=1}^n \omega_{Q_j} \right) \left( \prod_{j=1}^n 2 |U_x(Q_j)|^2 \omega_{Q_j}^{-1} (n_{Q_j} + 1) \right) \left[ 1 + (-1)^{n+1} \cos \left( 2 \sum_{j=1}^n \varphi_{Q_j} \right) \right], \quad (3.13)$$

where the  $x$  component of the Fourier-transformed relative displacement has been written in terms of its magnitude and phase  $\varphi_Q$ :

$$U_x(Q) = w_{<Qx} - (m_{<}/m_{>})^{1/2} w_{>Qx} e^{i\alpha_x a_{nn}} = |U_x(Q)| e^{i\varphi_Q}. \quad (3.14)$$

Writing  $\Sigma_n$  in Eq. (3.13) in terms of the magnitude and phase of  $U_x(Q)$  puts  $\Sigma_n$  in a form in which the quasiselection rule is manifest. An examination of the polarization vectors of phonons throughout the Brillouin zone reveals that the phases of optical and acoustical phonons are approximately  $0^\circ$  and  $-90^\circ$ , respectively. These approximate phases can be derived from either a simple diatomic linear lattice model or from more realistic three-dimensional models. Substitution of the phases in the cosine term of Eq. (3.13) yields the quasiselection rule that the fundamental reststrahl phonon prefers to split into final states containing an odd number of optical phonons (transition-matrix elements large). Final states containing an even number of optical phonons are less favored (transition-matrix elements small). Other statements of the quasiselection rule are possible. It is stated in terms of the optical phonons in the final states since, as will be demonstrated later, those final states containing primarily optical phonons dominate the absorption spectrum. The quasiselection rule places no restriction on the number of acoustical phonons in the final state.

For example, in the two-phonon region, the square-bracketed term containing the cosine factor in Eq. (3.13) becomes  $1 - \cos(180^\circ) = 2$  for an optical plus an acoustical final-state phonons. For two optical or two acoustical final-state phonons

this term is approximately zero. In the three-phonon region, three optical final-state phonons yield  $1 - \cos(540^\circ) = 2$  while two optical phonons plus an acoustical phonon yield approximately  $1 - \cos(360^\circ) = 0$ . Hence quasisallowed final states are one optical phonon plus any number of acoustical phonons, three optical phonons plus any number of acoustical phonons, etc.

Departures of the phases from their idealized values prevent the quasiselection rule from being exact, although typically there is a large degree of cancellation in the sum of the departures of the  $n$  phonons. For example, the exact two-phonon selection rule that the two final-state phonons cannot be on the same branch follows from the fact that the phases of the two phonons are equal and opposite because of equal and opposite momenta in spite of departures of the phases from their idealized values.

Crystal structures other than the rock-salt structure have not been examined yet. In other structures, such as the zinc-blende structure, the quasiselection rule derived here is not expected to be valid because the sum over nearest neighbors in Eq. (3.10) is expected to yield a different algebraic form than Eq. (3.13). The possibility of a different quasiselection rule in such crystals awaits further investigation.

The derivation of the phases of  $U_x(Q)$  for acoustical- and optical-phonon branches using a diatomic linear lattice is instructive. Consider a diatomic linear lattice having spring constant  $C$  and nearest-neighbor spacing  $a$  with light ions at positions  $2sa$  and heavy ions at positions  $(2s+1)a$ , where  $s$  is an integer. Analogous to Eq. (3.7) the displacements of the light and heavy ions for standing-wave normal modes are written

$$u_{2s} = m_{<}^{-1/2} w_{<} \cos(2sqa) \tag{3.15}$$

and

$$u_{2s+1} = m_{>}^{-1/2} w_{>} \cos[(2s+1)qa]. \tag{3.16}$$

The relative displacement of ions within a unit cell is

$$\begin{aligned} u_{2s} - u_{2s+1} &= m_{<}^{-1/2} \text{Re}[w_{<} - (m_{<}/m_{>})^{1/2} w_{>} e^{iqa}] e^{i2sqa} \\ &= m_{<}^{-1/2} |U_x(Q)| \cos(2sqa + \varphi_Q), \end{aligned} \tag{3.17}$$

where Re denotes the real part. The quantity within the square bracket of Eq. (3.17) is identical to  $U_x(Q)$  in Eq. (3.14). Components  $w_{<}$  and  $w_{>}$  of the normalized polarization vector are obtained from the equation of motion and have the ratio

$$w_{<}/w_{>} = [2C(m_{<})^{1/2}/(m_{>})^{1/2}] \cos qa / (2C - \omega^2 m_{<}), \tag{3.18}$$

where  $\omega$  is the frequency of the normal mode obtained from

$$\omega^2 = C/m_r \pm C [1/m_r^2 - (4/m_{<} m_{>}) \sin^2 qa]^{1/2}. \tag{3.19}$$

The displacements of the ions from their equilibrium positions are plotted at the top of Fig. 2 for acoustical and optical normal modes of a di-

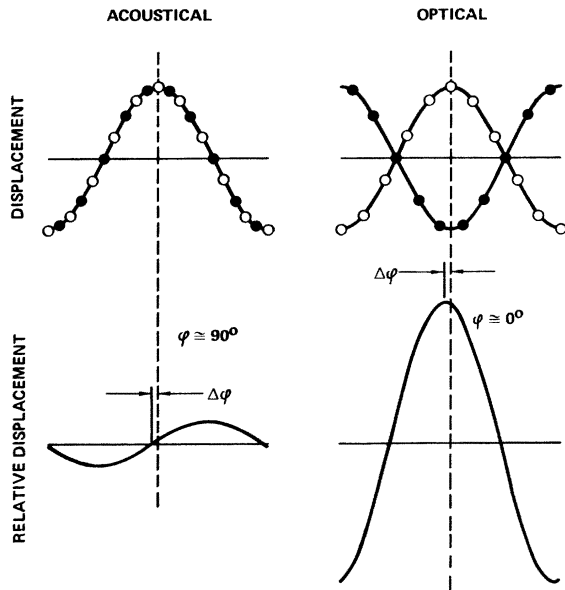


FIG. 2. Ion displacements for acoustical and optical normal modes of a linear diatomic lattice with ions of equal mass, upper curves. Relative displacement of ions, lower curves. The relative displacement curve for the optical mode is approximately in phase with the ion displacements, while the relative displacement curve for the acoustical mode is spatially displaced approximately 90°.

atomic chain having equal mass positive and negative ions. The relative displacements of the ions within each unit cell, obtained by taking the difference of heavy- and light-ion displacements and referencing the difference to the light-ion position, are plotted at the bottom of Fig. 2. Notice that the relative displacement curve for the optical mode is approximately in phase with the displacements, while the relative displacement curve for the acoustical mode is spatially displaced approximately 90° with the two relative displacement curves having a mutual spatial displacement of 90°. The departure  $\Delta\varphi$  of the spatial phases from the idealized values of 0° and -90° results from the lattice spacing being finite compared to the normal-mode wavelength.

In Fig. 3 the optical and the acoustical spatial phases are plotted as functions of the normal-mode wave number for four heavy- to light-ion mass ratios. The magnitude of the departure of the phase from the idealized value depends on the mass ratio and the position in the Brillouin zone. The idealized phase values are attained at the center and edge of the zone for all mass ratios, and are attained throughout the Brillouin zone for an infinite mass ratio. The maximum departure occurs for equal masses near the zone boundary.

Often the sum of the departures of the spatial phases from their idealized values is small or

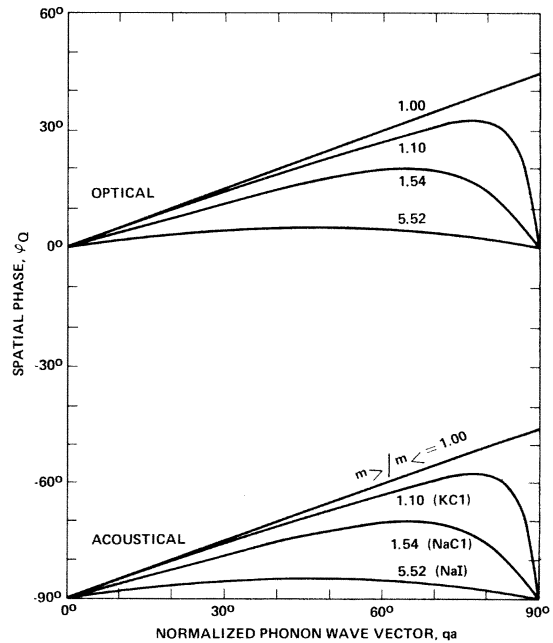


FIG. 3. Dependence of the spatial phase on the phonon wave vector and heavy- to light-ion mass ratio.

zero. In the diatomic linear lattice model the quasiselection rule is exact (sum departures zero) for the following cases: (i) For two final-state phonons the phase departures of the two phonons are equal and opposite because of momentum conservation. (ii) For crystals having positive and negative ions of equal mass, the linear dependence of the spatial phase on phonon momentum yields a zero sum for all numbers of final-state phonons if the momenta sum to zero. (For the less likely cases where three or more final-state phonons sum to an odd-numbered reciprocal-lattice vector, an exact violation of the quasiselection rule results.) (iii) For crystals having an infinite mass ratio between heavy and light ions there is zero deviation from the idealized phases.

More realistic three-dimensional models yield momentum and mass ratio dependent spatial phases similar to those in Fig. 3. Using polarization vectors from the deformable dipole model for NaI,<sup>18</sup> the following mean phases are obtained: 2.8°, 2.8°, and 3.9° for the optical modes and -74°, -71°, and -65° for the acoustical modes. These values for the optical modes agree with those in Fig. 3 for a linear diatomic lattice having the same mass ratio, although the departure of the phases of the acoustical modes from the idealized value of -90° is somewhat larger. A large degree of cancellation is again found in the sum of the phase departures, although the cancellation is now complete only for two final-state phonons on the same branch.

#### IV. CALCULATION OF THE ANHARMONIC CONTRIBUTION TO THE ABSORPTION COEFFICIENT

The perturbation-theory calculation of the relaxation frequency from Eqs. (3.9) and (3.13) is greatly simplified if the magnitude of  $U_x(Q_j)$  for a given branch is replaced by the Brillouin zone averaged value  $U_x(b_j)$ . (This is equivalent to neglecting phonon momentum conservation.) Assuming that this is valid and that the quasiselection rule is exactly satisfied, the extremely complicated momentum-dependent sum in Eq. (3.13) is reduced to a thermal- and frequency-weighted multiphonon density of states in which the phonon branches are kept distinct. For a quasilow combination of phonon branches, the contribution to  $\Sigma_n$  becomes

$$\begin{aligned} \Sigma_{b_1, \dots, b_n} &= 4N^{-n} |U_x(b_1)|^2 \cdots |U_x(b_n)|^2 \\ &\times \left( \sum_{\vec{q}_j} \omega_{\vec{q}_j}^{-1} (n_{\vec{q}_j} + 1) \right) \cdots \left( \sum_{\vec{q}_j} \omega_{\vec{q}_j}^{-1} (n_{\vec{q}_j} + 1) \right) \\ &\times \delta \left( \omega - \sum_{j=1}^n \omega_{\vec{q}_j} \right). \end{aligned} \quad (4.1)$$

The error resulting from taking the mean value of the magnitude of  $U_x(Q_j)$  is small if the magnitude is insensitive to position in the Brillouin zone. Magnitudes obtained from the linear diatomic chain model are plotted as a function of normal-mode wave number in Fig. 4 for four mass ratios. The assumption of a constant magnitude is best satisfied for the optical branch of crystals having a large mass ratio. Acoustical branches of crystals having equally massive positive and negative ions are most sensitive to the phonon wave vector. However, the error resulting from the strong dependence of  $|U_x(Q_j)|$  of acoustical branches on phonon wave vector is ameliorated by the following considerations: First, the region near the zone center contains only a small fraction of the Brillouin zone volume and there are no peaks in the acoustical-phonon density of states in this region. Second, as will be seen below, the relaxation frequency is dominated by final states containing primarily optical-branch phonons with final states containing primarily acoustical phonons being buried under lower-order combinations of optical-branch phonons.

Magnitudes of  $U_x(Q_j)$  similar to those in Fig. 4 are found using the deformable dipole model.<sup>18</sup> This model yields the root-mean-square magnitudes 0.589, 0.595, and 0.611 for the optical branches of NaI and 0.137, 0.188, and 0.221 for the acoustical branches. Using these magnitudes and assuming that the quasiselection rule is exactly satisfied, the relaxation frequency of NaI at 80 K has been calculated and is presented in Fig. 5. All derivatives of the potential were evaluated using the method of Eldridge and Howard.<sup>14</sup> For the fourth derivative, or greater, use of only the

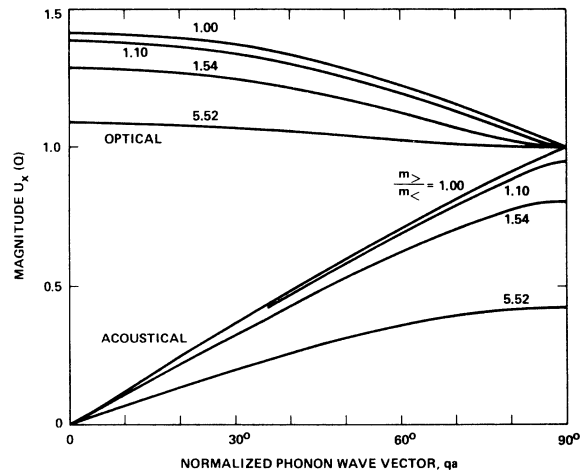


FIG. 4. Dependence of the magnitude of the Fourier-transformed relative displacement on the phonon wave vector and heavy- to light-ion mass ratio.

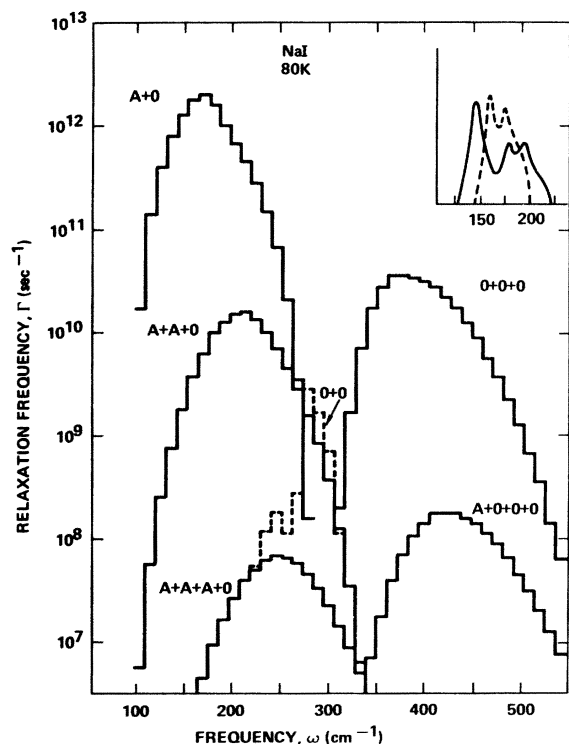


FIG. 5. Relaxation frequency of the fundamental reststrahl mode as a function of frequency. The dashed curve presents the quasiunallowed contribution from two optical phonons. Inset presents the spectral width function of the zero-momentum LO phonon at 300 K (solid curve) and 90 K (dashed curve). [Inset after Cowley, *et al.* (Ref. 20).]

Born-Mayer repulsive term yields equivalent results.<sup>4</sup>

The total relaxation frequency is the sum of the quasiallowed combinations in Fig. 5. To illustrate the validity of the quasiselection rule, the quasiunallowed combination of two optical-branch phonons has been calculated and is presented as a dashed curve in Fig. 5.<sup>12</sup> Notice that the spectrum is dominated by the two combinations A + O and O + O + O. Hence, there would be little loss in accuracy if contributions to  $\Gamma$  from final states containing more than one acoustical phonon were neglected. The peak in  $\Gamma$  from three optical phonons will be reflected in a peak in the absorption coefficient near this frequency.

The calculated absorption coefficient of NaI at 80 K is compared to experimental data from Harrington *et al.*<sup>3</sup> in Fig. 6. The frequencies of the experimental and theoretical three-phonon summation bands agree, although the theoretical curve is much sharper than the experimental curve. At room temperature the experimental peak is almost completely smoothed out while the room-temperature theoretical curve is nearly as strongly peaked

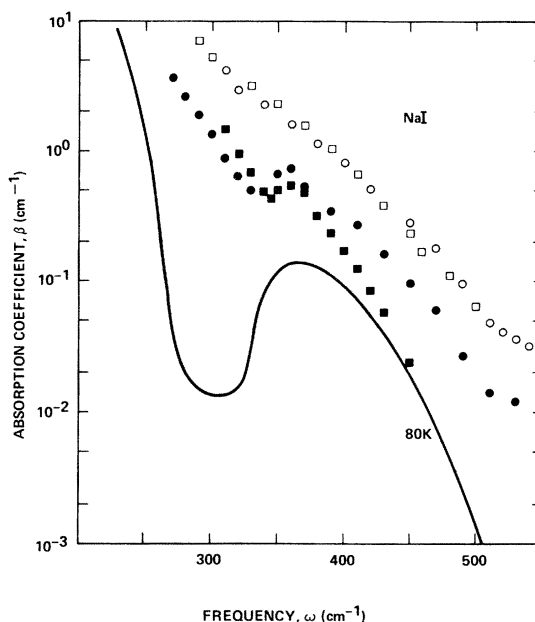


FIG. 6. Comparison of the 80-K theoretical absorption coefficient (solid curve) to the 80-K data (solid circles and squares). Open circles and squares present 300-K experimental data.

as the low-temperature curve. Using a density of states from a shell-model calculation of Cowley *et al.*<sup>19</sup> yields an even more strongly peaked curve at nearly the same frequency.

The increased width in the experimental peak is not due to violations of the quasiselection rule, but rather is thought to result from the linewidth of the final-state phonons. In calculating  $\Gamma$  in Fig. 5 it is tacitly assumed that the final-state linewidth is less than the histogram bin width of 11  $\text{cm}^{-1}$ . This is satisfied for the acoustical and some optical phonons at 80 K, but is not satisfied for longitudinal-optical phonons. The spectral width function of the  $q=0$ , LO phonon as calculated by Cowley *et al.*<sup>20</sup> is shown in the inset in Fig. 5. The large spectral width of the LO phonons broadens the O + A contribution to  $\Gamma$  on the high-frequency side and fills in the sharp dip between the two- and three-phonon regions. Beside broadening the 80-K theoretical peak, the strong temperature dependence of the spectral width function is thought to account for the disappearance of the distinct peak at room temperature.

Harrington *et al.*<sup>3</sup> observe that the three-optical-phonon peak is most pronounced in crystals having a large heavy- to light-ion mass ratio. Such crystals have frequency gaps in their phonon spectra. Consequently they have more structure in their multiphonon densities of states. This together with the facts that the idealized phase values are

more nearly attained and the magnitudes of the relative displacements are more nearly constant in the case of large mass ratios, favors structure in the multiphonon absorption coefficient.

### V. VERTEX RENORMALIZATION FACTORS

Sparks and Sham<sup>4</sup> treat higher-order diagrams involving intermediate-state phonons as a vertex renormalization factor  $\Lambda_n$  to the simple vertex where the fundamental phonon splits directly into  $n$  final-state phonons. The contribution of these diagrams to the relaxation frequency can be explicitly calculated using a more general quasiselection rule and the above method of calculation where mean values of  $|U_x(Q)|$  are used. Perturbation-theory analysis of the general  $n$ -phonon vertex yields a cosine factor similar to that in Eq. (3.13) from which a more general quasiselection rule is derived that quasisallowed vertices contain an even number of optical phonons. In this more general case incoming as well as outgoing phonons are counted and the number and wave vectors of the incoming phonons are not restricted. The previously considered case of a single zero-momentum, TO incoming phonon is a special case.

For three final-state phonons there is only one higher-order diagram containing an intermediate-state phonon. This diagram is sketched in Fig. 7. At the first vertex the fundamental phonon must split into an optical phonon plus an acoustical phonon with splitting into two optical or two acoustical phonons being unallowed by the quasiselection rule. The intermediate-state phonon, labeled by  $m$ , can be either the optical or the acoustical phonon with the final-state phonon, labeled by 1, being the other.

In the case where the intermediate-state phonon is the optical phonon, the above general quasiselection rule requires that it split into an optical plus an acoustical phonon at the second vertex. Hence the final state consists of one optical plus two acoustical phonons.

In the other case where the intermediate-state phonon is the acoustical phonon, this phonon is allowed by the general quasiselection rule to decay into either two optical phonons or two acoustical phonons at the second vertex. Hence the two possible final states in this case are three optical phonons or one optical phonon plus two acoustical phonons.

These two quasisallowed final states for the higher-order diagram are exactly the same as for the simple vertex where the fundamental phonon splits directly into three final-state phonons. Therefore the quasiselection rule for the simple

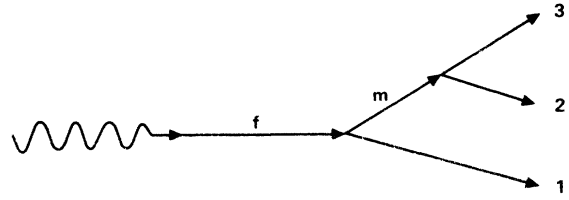


FIG. 7. Higher-order three-phonon diagram involving an intermediate-state phonon.

vertex remains valid overall even though two of the final-state phonons came from an intermediate-state phonon. Similarly for more than three final-state phonons, an examination of the higher-order diagrams in these cases reveals that the quasiselection rule for the simple vertex remains valid overall as long as the general quasiselection rule is satisfied at every intermediate-state vertex.

The ratio of the transition-matrix element for the higher-order diagram in Fig. 7 to the simple vertex is<sup>4,21</sup>

$$\frac{\langle f | \mathcal{H}'_3 | i \rangle}{\langle f | \mathcal{H}_3 | i \rangle} = \sum_{b_m} \frac{4\omega_m V(fQ_m Q_1) V(Q_m Q_2 Q_3)}{3\hbar [(\omega - \omega_{Q_1})^2 - \omega_{Q_m}^2] V(fQ_1 Q_2 Q_3)}, \quad (5.1)$$

where for fixed initial and final states it is only necessary to sum over the branches of the intermediate-state phonon denoted by  $m$ . Evaluating the vertices, Eq. (5.1) becomes

$$\begin{aligned} \frac{\langle f | \mathcal{H}'_3 | i \rangle}{\langle f | \mathcal{H}_3 | i \rangle} &= \frac{4}{9m_c} \frac{(\phi^{(3)})^2}{\phi^{(4)}} \\ &\times \sum_{b_m} \frac{\alpha(fQ_m Q_1) \alpha(Q_m Q_2 Q_3)}{[(\omega - \omega_{Q_1})^2 - \omega_{Q_m}^2] \alpha(fQ_1 Q_2 Q_3)}, \end{aligned} \quad (5.2)$$

where

$$\alpha(Q_1, \dots, Q_n) = 2 |U_x(Q_1)| \cdots |U_x(Q_n)|$$

for quasisallowed diagrams and approximately zero otherwise. For the final state consisting of three optical phonons the intermediate-state phonon is an acoustical phonon. Approximating the square-bracketed frequency term by  $4\omega_f^2$  and multiplying by 3 for the three quasisallowed acoustical branches yields

$$\begin{aligned} \frac{\langle f | \mathcal{H}'_3 | i \rangle}{\langle f | \mathcal{H}_3 | i \rangle} &= \frac{2}{3} \frac{(\phi^{(3)})^2}{\phi^{(4)}} \frac{|U_x(A)|^2}{m_c \omega_f^2} \\ &= 1.5 \times 10^{-2} \text{ for NaI.} \end{aligned} \quad (5.3)$$

Hence the vertex correction factor is  $\Lambda_3 = 1.1015$  which implies that the quantity  $\xi$  defined by Sparks and Sham<sup>4</sup> is  $\xi = 0.020$ . Rather than explicitly evaluating the vertex corrections to the higher-order diagrams, this quantity is used to obtain  $\Lambda_4 = 1.04$



and  $\Lambda_s = 1.08$ . These corrections are negligible. They are much smaller than those obtained by McGill *et al.*<sup>6</sup> and are even smaller than those obtained by Sparks and Sham.<sup>4</sup>

Corrections arising from confluence diagrams in the multiphonon region are still smaller. Since confluence diagrams contain predominantly incoming acoustical phonons, the overall quasiselection rule for allowed final states remains valid.

## VI. CONCLUSIONS

Many of the basic assumptions and approximations made by Sparks and Sham<sup>4</sup> remain in the present paper, although several improvements have been made and new results have been obtained. These assumptions and approximations are summarized as follows: (i) As justified by Sparks and Sham,<sup>4</sup> the perturbation-theory approach is assumed valid. (ii) Only the anharmonic-lattice mechanism is included in the calculation of the absorption coefficient. It is argued in Sec. II that the inclusion of the higher-order dipole-moment mechanism is expected to only change the strength of the interaction, leaving the phonon dynamics and the quasiselection rule unchanged. (iii) A nearest-neighbor central-force potential is assumed. Use of only the Born-Mayer repulsive term for three, or more, phonons is convenient, but not essential. (iv) The lifetimes of final-state phonons are taken to be infinite in the calculated curves. However, evidence is presented that the large spectral width of optical phonons, especially at room temperature, contributes considerable broadening to the theoretical curves bringing the calculated line shape of the three-optical-phonon summation band into better agreement with experiment. (v) An error in the Sparks and Sham paper,<sup>4</sup> on which the use of the central-limit theorem was based, has been corrected. In the present paper multiple sums over phonon modes have been approximated by Brillouin zone averages in which the phonon branches are kept distinct. It is

shown in Sec. IV that this is a reasonable approximation, especially for optical phonons which dominate the spectrum.

The results of this paper are: (i) A quasiselection rule is derived that infrared absorption in alkali halide crystals tends to create final states having an odd number of optical phonons. This quasiselection rule follows from the observation that the relative motion between ions in a unit cell is approximately spatially in phase with the ion motion for optical modes, while the acoustical modes are approximately  $90^\circ$  spatially out of phase with the ion motions. (ii) The quasiselection rule explains the observations of Harrington *et al.*<sup>3</sup> of a three-optical-phonon summation-band peak in the absorption coefficient with no corresponding peak being observed at two or four optical phonons. (iii) Using a constant magnitude Fourier-transformed relative displacement greatly reduces the effort of the perturbation-theory calculation. This approximation is justified by the demonstration that, at least for optical modes, the magnitude of the Fourier-transformed relative displacement is insensitive to the phonon momentum for a given branch. This allows an extremely complicated momentum-dependent sum over phonon modes to be reduced to an easily evaluated thermally and frequency-weighted density of states in which the phonon branches are kept distinct. (iv) A more general quasiselection rule allows easy evaluation of vertex correction factors from higher-order diagrams containing intermediate-state phonons. These factors are found to be smaller than those estimated by Sparks and Sham,<sup>4</sup> and, in agreement with Sparks and Sham, are found to be negligible.

## ACKNOWLEDGMENTS

I thank Dr. M. Hass for bringing the data of Dr. J. A. Harrington to my attention. Helpful discussions with Dr. M. Hass, Dr. J. A. Harrington, and Dr. M. Sparks are gratefully acknowledged.

\*Research supported by the Advanced Research Projects Agency of the Department of Defense and monitored by the Defense Supply Service, Washington, D.C. under Contract No. DAHC15-73-C-0127.

<sup>1</sup>See, for example, *Proceedings of the International Conference on the Optical Properties of Highly Transparent Solids, 1975*, edited by B. Bendow and S. S. Mitra (Plenum, New York, 1975).

<sup>2</sup>T. F. Deutsch, *J. Phys. Chem. Solids* **34**, 2091 (1973).

<sup>3</sup>J. A. Harrington, C. J. Duthler, F. W. Patten, and M. Hass, *Solid State Commun.* **18**, 1043 (1976).

<sup>4</sup>M. Sparks and L. J. Sham, *Phys. Rev. B* **8**, 3037 (1973).

<sup>5</sup>D. L. Mills and A. A. Maradudin, *Phys. Rev. B* **8**, 1617 (1973).

<sup>6</sup>T. C. McGill, R. W. Hellwarth, M. Mangir, and H. V. Winston, *J. Phys. Chem. Solids* **34**, 2105 (1973).

<sup>7</sup>B. Bendow, S. C. Ying, and S. P. Yukon, *Phys. Rev. B* **8**, 1679 (1973).

<sup>8</sup>K. V. Namjoshi and S. S. Mitra, *Phys. Rev. B* **9**, 815 (1974).

<sup>9</sup>L. L. Boyer, J. A. Harrington, M. Hass, and H. B. Rosenstock, *Phys. Rev. B* **11**, 1665 (1975).

<sup>10</sup>M. Lax and E. Burstein, *Phys. Rev.* **97**, 39 (1955).

<sup>11</sup>R. Loudon, *Phys. Rev.* **137**, A1784 (1965).

- <sup>12</sup>C. J. Duthler and M. Sparks, *Phys. Rev. B* 9, 830 (1974).
- <sup>13</sup>C. Smart, G. R. Wilkinson, A. M. Karo, and J. R. Hardy, in *Lattice Dynamics*, edited by R. F. Wallis (Pergamon, Oxford, England, 1965), p. 387.
- <sup>14</sup>J. E. Eldridge, *Phys. Rev. B* 6, 1510 (1972); J. E. Eldridge and R. Howard, *ibid.* 7, 4652 (1973).
- <sup>15</sup>P. N. Keating and G. Rupprecht, *Phys. Rev.* 138, A866 (1965).
- <sup>16</sup>R. A. Cowley, *Adv. Phys.* 12, 421 (1963).
- <sup>17</sup>M. Sparks, *Phys. Rev. B* 10, 2581 (1974).
- <sup>18</sup>A. M. Karo and J. R. Hardy, *Phys. Rev.* 129, 2024 (1963).
- <sup>19</sup>R. A. Cowley, W. Cochran, B. N. Brockhouse, and A. D. B. Woods, *Phys. Rev.* 131, 1030 (1963).
- <sup>20</sup>E. R. Cowley and R. A. Cowley, *Proc. R. Soc. A* 287, 259 (1965); A. D. B. Woods, B. N. Brockhouse, R. A. Cowley, and W. Cochran, *Phys. Rev.* 131, 1025 (1963).
- <sup>21</sup>M. Sparks, Xonics, Inc. Technical Report, Dec. 1972, Contract No. DAHC 15-72-C-0129 (unpublished).